Journal of CO_2 Utilization 16 (2016) 375–383

Contents lists available at ScienceDirect

Journal of CO_2 Utilization

journal homepage: www.elsevier.com/locate/jcou

Electrochemical promotion and characterization of PdZn alloy catalysts with K and Na ionic conductors for pure gaseous CO_2 hydrogenation

J. Díez-Ramírez*, P. Sánchez, J.L. Valverde, F. Dorado

Departamento de Ingeniería Química, Facultad de Ciencias y Tecnologías Químicas, Avenida Camilo José Cela 12, 13071 Ciudad Real, Spain

ARTICLE INFO

Article history:
Received 17 March 2016
Received in revised form 29 August 2016
Accepted 29 September 2016
Available online 3 October 2016

Keywords:
Electrochemical promotion of catalysis (EPOC)
CO2 hydrogenation
PdZn alloy
Methanol production

ABSTRACT

A PdZn alloy has been used for the first time as a catalytic electrochemical film for CO_2 hydrogenation. Three different electrochemical systems were prepared to study the influence of the Pd/Zn ratio and the presence of potassium and sodium ions. These catalysts were characterized by XRD, SEM and cyclic voltammetry and then tested in the hydrogenation of CO_2 at three different H_2/CO_2 feed ratios (3, 9 and 39) and three temperatures (300, 320 and 340 °C) with electrochemical promotion by Na^+ and K^+ ions. CH_3OH and CO were the only two products detected. During the electrochemical promotion, a low quantity of ions increases the formation rate of CH_3OH and a high quantity leads to the poisoning of the PdZn active sites. The catalysts which have palladium and the palladium-zinc alloy in their structure show an electrophilic behavior in the CO formation and when only the alloy is formed in the catalyst, the CO has the same behavior found for the methanol. Apparent Faradaic efficiency values above 1000 were obtained under the different conditions tested.

1. Introduction

The valorization of carbon dioxide to desirable compounds is one of the targets of the scientific community in general, especially considering the recent increase in the emission of this pollutant, which is well-known as the most important greenhouse gas. The carbon dioxide molecule is practically unreactive but it is unquestionably a major carbon source. Therefore, the challenge for scientists is to transform CO_2 into chemical compounds such as hydrocarbons, alcohols, aldehydes, etc. [1–4].

Hydrogenation of carbon dioxide is one of the possible ways to valorize this compound and this reaction continues to be studied in the field of conventional catalysis [5–7]. Indeed there are several pilot plants in Japan [8,9] and a commercial CO_2-to-methanol recycling plant in Iceland [10]. The wide range of products that are allowed in the general equation (Eq. (1)) means that high conversion and high selectivity towards the desired product are the two most important parameters in this reaction. In this sense, promotion by alkali has been reported to be an effective approach to control the activity and selectivity of a catalyst [11]. Although this promotion could be carried out by conventional catalysis, electrocatalysis allows control of this alkali promotion by varying the polarization of a catalyst-electrode through the effect of electrochemical promotion of catalysis (EPOC), also known as non-Faradaic electrochemical modification of catalytic activity (the NEMCA effect).

$$xCO_2 + (2x - z + y/2)\ H_2 \leftrightarrows C_xH_yO_z + (2 - z)\ H_2O \quad (1)$$

The NEMCA effect was first observed by Stoukides and Vayenas [12]. The effect is based on the controlled migration of promoting ions (i.e., O^{2-}, Na^+, K^+ or H^+) from an electroactive support, such as β"-Al_2O_3 (K^+ and Na^+ conductor), YSZ (yttrium-stabilized-zirconia, an O^{2-} conductor), SZY ($SrZr_{0.95}Yb_{0.05}O_{3\pm d}$, a H^+ conductor), CZY ($CaZr_{0.9}In_{0.1}O_{3-\alpha}$, a H^+ conductor) or BZY ($BaZr_{0.8}Y_{0.2}O_{3\pm\delta}$, a H^+ conductor), to the catalytic metal/gas interface. The migration of the ions allows in situ control of the catalytic behavior of the system by changing the binding strength of chemisorbed species and reaction intermediates [13,14].

Very few EPOC studies have been devoted to the reaction discussed here and the vast majority was previously summarized by our group [15]. A total of fourteen such papers have been published, including the most recent paper [16], and this total is a very low compared to other fields of research.

The most commonly used active metals are Cu, Pd, Pt, Ru and Rh supported on Na-β″Al_2O_3 [17], K-β″Al_2O_3 [18–21], YSZ [17,20,22–27], or SZY [28]. The most common products are carbon monoxide and methane—except for the works by Esperanza et al. [18,19,25], where alcohols and hydrocarbons were obtained on

* Corresponding author.
E-mail addresses: Javier.Diez@uclm.es, javi74.dr@gmail.com (J. Díez-Ramírez).

http://dx.doi.org/10.1016/j.jcou.2016.09.007
2212-9820/

working under realistic post-combustion CO_2 capture exiting gas compositions on a bench-scale plant. The novelty of the work described here is the use of a PdZn alloy as the catalyst-electrode in the electrocatalytic system. The PdZn alloy has previously been studied in conventional catalysis by our group [29,30] and it has also been extensively studied for the steam reforming of methanol [31–36]. This catalyst showed interesting properties in terms of the selectivity and activity to methanol. The study reported here is the first in which the only two products obtained in a pure gaseous hydrogenation of CO_2 in EPOC studies are carbon monoxide and methanol, as described by the following equations:

$$CO_2 + H_2 \leftrightarrows CO + H_2O \quad (2)$$

$$CO_2 + 3H_2 \leftrightarrows CH_3OH + H_2O \quad (3)$$

In this work three different electrocatalytic systems (PdZn/K-βAl_2O_3/Au, PdZn/K-βAl_2O_3/Au with a different PdZn molar ratio and PdZn/Na-βAl_2O_3/Au) were studied by different characterization techniques and with catalytic activity experiments under electrochemical promotion conditions. The influence of the Pd/Zn molar ratio on the formation of the PdZn alloy or the way in which promotional ions (K^+ or Na^+) affect the electrochemical results were studied. Moreover, an in-depth electrochemical study was carried out with PdZn/K-βAl_2O_3/Au using a Pd/Zn molar ratio of 1.

2. Experimental

2.1. Electrochemical cell preparation

Each electrochemical cell consisted of a 19-mm-diameter, 1-mm-thick (K, Na)- β"Al_2O_3 (Ionotec) pellet as the solid electrolyte. In each electrochemical cell the Au counter and reference electrodes were first deposited on one side of the electrolyte by annealing a gold organometallic paste (Fuel Cell Materials ref-231001) in two correlative stages, firstly at 300 °C for 1 h and secondly at 800 °C for 2 h (heating ramps of 5 °C/min). The PdZn catalyst films were subsequently deposited by impregnation. Thus, two solutions of palladium(II) nitrate [$Pd(NO_3)_2 \cdot xH_2O$, Aldrich] and zinc nitrate 6-hydrate [$Zn(NO_3)_2 \cdot 6H_2O$, Panreac] were prepared. The first solution was 0.1 M in both metals (Pd/Zn molar ratio of 1), whereas the second one was 0.1 M in palladium with a Pd/Zn molar ratio of 0.13 (the best molar ratio found in a previous study carried out with conventional catalysts [29]). In each impregnation, 20 μl of solution were added and then the sample was calcined at 500 °C with a heating rate of 5 °C/min. After all of the required impregnations (36 for each cell) had been completed, different quantities of metals were deposited in ~1.5 cm^2 areas. The description and nomenclature of each electrochemical catalyst are summarized in Table 1, along with the different palladium and zinc weights, particle sizes and active surface area of palladium and PdZn alloy. The active surface mol were calculated in each case taking into account the total amount of deposited mol of each metal, the EDX measurements, the particle diameter and dispersion values for each compound, which were estimated from XRD via the Scherrer equation. For the calculation of product formation rates, it has been considered that the methanol is preferentially produced on the PdZn active sites whereas the carbon monoxide is produced on both active sites [30].

2.2. Electrochemical catalyst characterization

A temperature-programed reduction (TPR) experiment was carried out in situ during the reduction of the catalysts under a stream of hydrogen (10 vol%) diluted with nitrogen at a flow rate of 25 ml min^{-1}. The temperature was increased at a heating rate of 1.3 °C min^{-1} up to 500 °C. During the TPR, the H_2 consumption was continuously monitored by a thermal conductivity detector, whereas the in-plane PdZn film surface electrical resistance between two points separated by 1 cm was measured using a digital multimeter. XRD analyses were carried out on a Philips X'Pert instrument using nickel-filtered Cu-Kα radiation. Samples were scanned at a rate of 0.02° $step^{-1}$ over the range $5° \leq 2\theta \leq 90°$ (scan time = 2 s $step^{-1}$). The morphology of the different catalyst films was evaluated using a Phenom Pro X scanning electron microscope (SEM). This instrument was equipped with an Energy Dispersive X-ray Spectroscopy (EDX) analyzer to determine the average composition of the samples. Cyclic voltammetry studies were carried out using a Voltalab PGZ 301 potentiostat-galvanostat (Radiometer Analytical). The potential was scanned between 2 and 2.5 V (starting potential) and −2 V at a scan rate of 50 mV s^{-1}. The current density generated by the applied cyclic polarization was recorded as a function of the applied potential relative to the counter-reference electrode.

2.3. Catalytic activity measurements

The experimental setup was described in detail in a previous publication [37]. Reaction gases were Praxair certified standards of CO_2 (99.999% purity), H_2 (99.999% purity) and N_2 (99.999% purity). The gas flows were controlled by a set of calibrated mass flowmeters (Brooks 5850 E and 5850 S).

Prior to reaction, catalysts were reduced as explained above for the TPR experiment. The catalytic runs were carried out at atmospheric pressure. The total flow rate was of 120 ml min^{-1}, which is sufficiently high to avoid any mass transfer limitation phenomena. Three H_2/CO_2 ratios were selected: 3 (75% H_2 and 25%

Table 1
Summary of the different PdZn based electrochemical catalyst.

Nomeclature	PdZn/Na	PdZn/K	PdZn0.13/K
Description	PdZn/Na-βAl_2O_3/Au	PdZn/K-βAl_2O_3/Au	PdZn/K-βAl_2O_3/Au
Pd/Zn molar ratio	1	1	0.13
Total Pd weight (mg)	7.66	7.66	7.66
Total Zn weight (mg)	4.71	4.71	36.22
PdZn alloy particle size after reaction (nm)	78.0	84.5	52.6
Pd particle size after reaction (nm)	72.6	59.3	–
ZnO particle size after reaction (nm)	–	–	60.4
N_{Pd} (active mol of metallic palladium)	6.57×10^{-7}	9.71×10^{-8}	–
N_{PdZn} (active mol of PdZn alloy)	9.00×10^{-7}	1.88×10^{-6}	3.25×10^{-6}
$N_{Pd+PdZn}$ (total active mol)	1.56×10^{-6}	1.98×10^{-6}	3.25×10^{-6}

CO_2), 9 (90% H_2 and 10% CO_2) and 39 (97.5% H_2 and 2.5% CO_2). The experiments were carried out at three temperatures (300, 320 and 340 °C). Reactant and product gases were on-line analyzed using a micro gas-chromatograph (Varian CP-4900) equipped with two columns (Molsieve and Poraplot Q column) and two thermal conductivity detectors (TCD). The detected reaction products were CO and CH_3OH. The error in the carbon atom balance did not exceed 1%. In order to carry out the electrochemical promotion (EPOC) experiments, the three electrodes (working, counter and reference) were connected to a Voltalab PGZ 301 potentiostat-galvanostat (Radiometer Analytical) using gold wires. The CO_2 conversion and the CO and CH_3OH selectivities were calculated as follows (Eqs. (4)–(6)):

$$CO_2 conversion(\%) = \frac{F^0_{CO_2} - F_{CO_2}}{F^0_{CO_2}} x100 \quad (4)$$

$$COselectivity(\%) = \frac{F_{CO}}{F^0_{CO_2} - F_{CO_2}} x100 \quad (5)$$

$$CH_3OHselectivity(\%) = \frac{F_{CH_3OH}}{F^0_{CO_2} - F_{CO_2}} x100 \quad (6)$$

2.4. EPOC parameters

In the electrochemical promotion of catalysis there is a correspondence between the different potentials applied and the amount of ions electrochemically transferred to the metal film, thus modifying the adsorption of the different gases and ultimately the catalytic behavior. Several different parameters are commonly used to quantify the electropromotional effect:

- The rate enhancement ratio, ρ, defined by Eq. (7):

$$\rho = r/r_0 \quad (7)$$

where r is the electropromoted catalytic rate and r_0 is the unpromoted rate.

- The apparent Faradaic efficiency, Λ, defined by Eq. (8):

$$\Lambda_i = \Delta r_{catalytic}/(I/F) \quad (8)$$

where $\Delta r_{catalytic}$ is the current- or potential-induced observed change in catalytic rate and I is the applied current. For this work, it implies:

$$\Lambda_{CO} = 2\Delta r_{CO}/(I/F) \quad (9)$$

$$\Lambda_{CH3OH} = 6\Delta r_{CH3OH}/(I/F) \quad (10)$$

where Δr_{CO} and Δr_{CH3OH} are in mol/s.

For the cyclic voltammetry studies, the corresponding coverage of potassium and sodium species established on the PdZn surface for each scan can be calculated according to Faraday's law (Eq. (11)) by integration of the current density versus time or, equivalently, versus potential curves obtained for the cathodic and anodic scan, respectively.

$$\theta_{KorNa} = \int \frac{I}{FN} dt = \frac{A}{F} \int j dt \quad (11)$$

where I is the current, F is the Faraday constant, N is the surface mol (mol of active sites) of the PdZn catalyst electrode, A is the superficial surface area of the electrode/electrolyte interface and *j* is the current density.

3. Results and discussion

3.1. Electrochemical catalyst characterization

The variation in the surface electrical resistance of the PdZn catalyst film and the H_2 consumption rate during a temperature programed reduction experiment (TPR) for the PdZn/K sample is shown in Fig. 1. Significant differences were not detected between the three electrochemical catalysts in the TPR experiment. At the beginning of the experiment, the PdZn film showed a very high electrical resistance (~23.7 MΩ). The decrease in the electrical resistance started at around 60 °C, when the first peak appeared in the TPR analysis. This peak was attributed to the reduction of PdO to metallic palladium [32]. The electrical resistance then stabilized around 4 Ω (See enlargement in Fig. 1). The second peak (450 °C) was related to the formation of the PdZn alloy [29,32], which is the active phase responsible for the formation of methanol.

The XRD patterns of the samples PdZn/Na, PdZn/K and PdZn0.13/K are shown in Fig. 2. The main peaks observed for the samples with a Pd/Zn molar ratio of 1 were those of metallic palladium (JCPDS 87-0645) and PdZn alloy (JCPDS 06-0620). The other small peaks that appeared were related to the solid electrolytes (JCPDS 02-0921). In the case of the sample PdZn0.13/K, which has a lower Pd/Zn molar ratio and therefore a higher zinc concentration in the impregnating solution, peaks corresponding to ZnO crystals were observed (JCPDS 80-0075) while the metallic palladium peaks were not. A difference in the intensities of the peaks was observed for the samples PdZn/K and PdZn/Na: for the latter the peaks due to the metallic palladium were higher and those for the PdZn alloy were lower. The intensities of the peaks are related to the amount of these species present [29,38]. This situation is consistent with EDX mapping analysis on SEM images (Fig. 3d). The sample PdZn/Na showed the highest Pd percentage even though PdZn/Na and PdZn/K samples should have the same quantity of palladium in the film. This discrepancy could be due to the position of the metallic palladium particles. These particles could be hidden in the pores of the film structure of the PdZn/K sample but located on the surface for the PdZn/Na sample. Such a phenomenon would have a consequence on the catalytic behavior, with the PdZn/Na sample being more active for carbon monoxide production due to the higher level of metallic palladium particles exposed. SEM images (Fig. 3a–c), all at

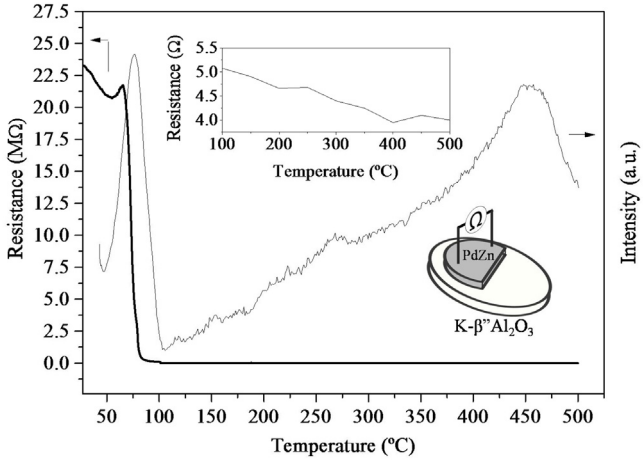

Fig. 1. TPR profile and variation of the PdZn surface electrical resistance with temperature.

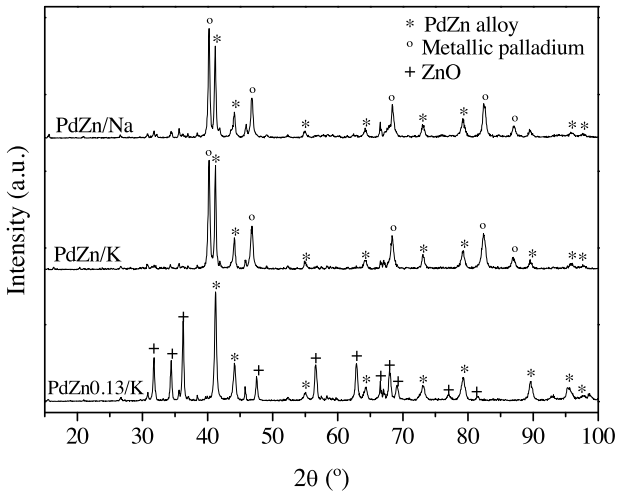

Fig. 2. XRD profile of PdZn/K, PdZn0.13/K and PdZn/Na samples after reduction.

a resolution of 30 μm, showed the different external morphologies of the catalyst films. The sample PdZn/Na (Fig. 3a) contained more holes and cavities in a similar way to the sample PdZn/K (Fig. 3b). However, the surface of the sample PdZn0.13/K is very different as it seems less compact, rougher and it contains small holes. This morphology allows particles to be hosted within a high surface area. Therefore, one would expect the dispersion for this catalyst to be higher.

The results of the cyclic voltammetry study are represented in Fig. 4. The cathodic peaks, which appear with the application of decreasing potentials, are related to species formed on the surface of the catalyst when the ions of the electroactive support migrate to the catalyst interface and react with the reactants. The anodic peaks, which appear with the application of increasing potentials, are related to the decomposition of these species. The voltammetry analysis for each sample at 300 °C with a feed composition of 90% H_2 and 10% CO_2 and a total flow rate of 120 ml min^{-1} are shown in Fig. 4a. The low intensity shown by the sample PdZn/K is related to the formation of only low levels of species on the surface. In contrast, the sample PdZn/Na showed the highest intensity, probably due to the high capacity of this sample to capture reactants on the surface and form Na compounds such as sodium carbonate [39,40]. Moreover, this high capacity to capture reactants on the surface could lead to deactivation of the active sites where these species are formed and this could therefore reduce the activity of the catalyst [39]. This possibility is supported by measurement of the potassium and sodium coverage (θ_K and θ_{Na}) (see Table 2). The marked difference between the formation and decomposition scan rates for the sample PdZn/Na suggests that decomposition of the formed species does not occur. These species remain on the surface of the catalyst film and block the active sites. The formation and decomposition scans for the samples PdZn/K and PdZn0.13/K are very similar (the small differences can be ascribed to the error inherent in the area integration). Therefore, a reversible promotional phenomenon was observed during cyclic voltammetry at all temperatures.

Another point that should be highlighted is the potential at which the highest cathodic peak was obtained. These values were −0.25 V, −0.75 V and −1 V for PdZn/K, PdZn0.13/K and PdZn/Na, respectively. This potential increased with temperature in each case (not shown here). At higher temperatures the same effect was observed with lower electricity consumption, as higher temperatures improve the migration of ions, thus increasing the electrolyte ionic conductivity with a concomitant increase in the number of available potassium storage sites. High temperature also increases the number of species formed. A cyclic voltammogram

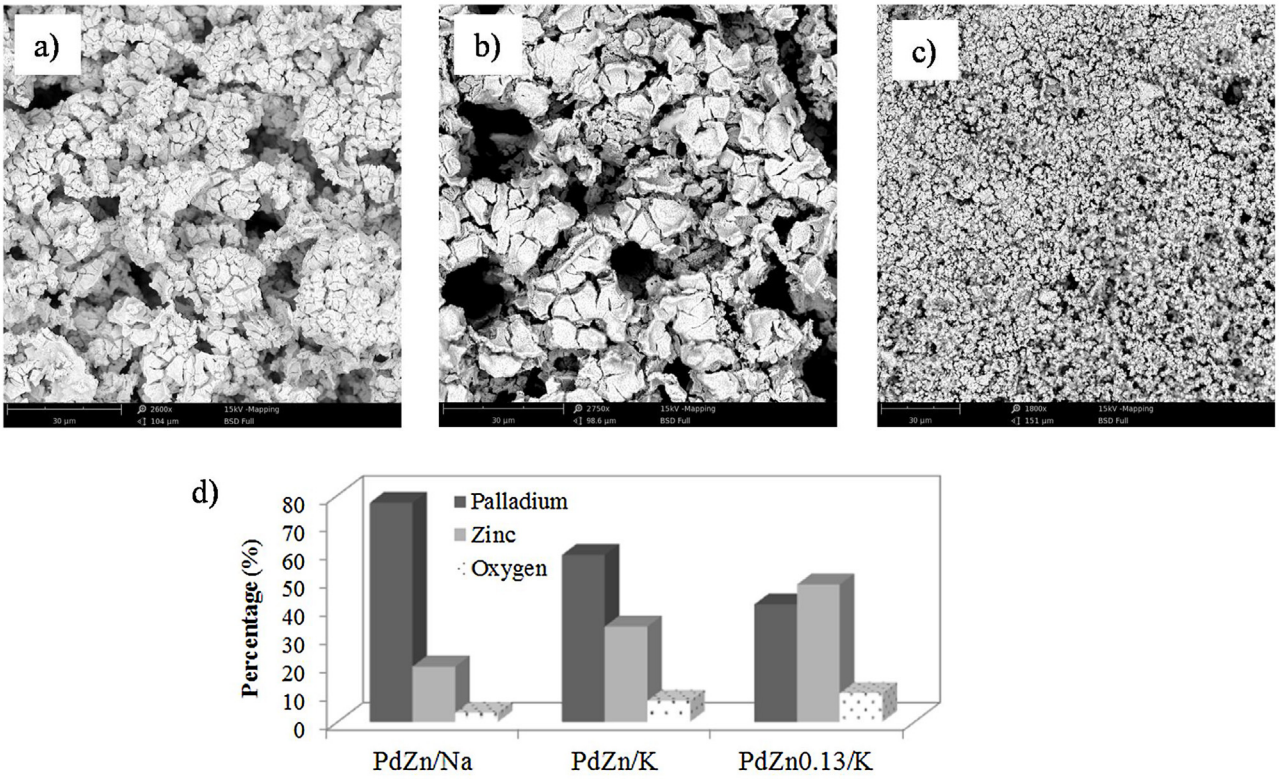

Fig. 3. SEM images of catalysts a) PdZn/K b) PdZn/Na and c) PdZn0.13/K. The EDX mapping composition is also included in d) for each sample.

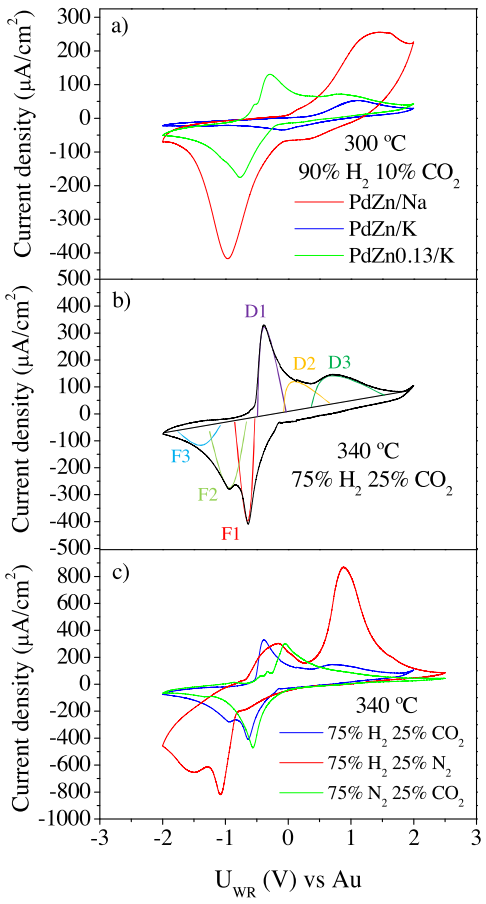

Fig. 4. Cyclic voltammograms recorded over a) PdZn/K (blue), PdZn/Na (red) and PdZn0.13/K (green) at 300 °C under conditions of 10% CO_2 and 90% H_2; b) PdZn0.13/K at 340 °C under 25% CO_2 and 75% H_2; and c) PdZn0.13/K under different conditions: 25% CO_2 and 75% H_2 (blue), 25% N_2 and 75% H_2 (red) and 25% CO_2 and 75% N_2 (green). (For interpretation of the references to colour in this figure legend, the reader is referred to the web version of this article.)

for the sample PdZn0.13/K at 340 °C is shown in Fig. 4b, where the cathodic and anodic peaks reach the highest values with 75% H_2/25% CO_2 because, under these conditions, there is a greater quantity of CO_2 available, which is responsible for the formation of the cathodic peaks. These cathodic peaks. In an effort to understand which species are formed, these peaks were identified and denoted with the letters F (Formation of species) and D (Decomposition of species). Three peaks appear in both sides of the cyclic voltammogram. Two additional experiments, in which both reactants were combined with N_2, were carried out at 340 °C (Fig. 4c) in order to establish a correspondence between the position of the peaks and the identity of the phases formed as a result of the potassium pumping. The peaks observed for 75% H_2 and 25% N_2 appeared at lower potentials (−1 V and −1.5 V), while the peak for 75% N_2 and 25% CO_2 appeared when the potassium ions were transferred to the PdZn film (~0.5 V). Therefore, the formation of peak F1 is related to carbonate species (potassium carbonate and bicarbonate) and the peaks F2 and F3 to hydrogen storage as potassium hydrides. D1 and D3 were attributed to the decomposition of these hydrides and D2 to the decomposition of carbonates. This assignment is consistent with data reported in literature. Thus, a similar study was carried out by Esperanza et al. [41] with CO_2 and O_2 in order to identify the compounds formed when a cathodic peak appears. The formation of these compounds has been also reported in other works: potassium carbonates were detected by XPS under similar reaction conditions [42,] as well as potassium bicarbonates due to the formation of water during the reaction [43]. In addition, in another work, the formation of potassium carbonate and potassium bicarbonate was observed and confirmed by FTIR measurements [44].

Table 2
Coverage of potassium and sodium species in Fig. 4a.

	PdZn/Na	PdZn/K	PdZn0.13/K
Decomposition scan	1.30·10-3	2.46·10-4	5.89·10-4
Formation scan	2.42·10-3	2.70·10-4	5.76·10-4
Relative change (%)	46.3	8.8	2.2

3.2. Effect of the gas flow rate

The effects of the gas flow rate on the CO_2 reaction rate, CO_2 conversion and selectivity to CO and CH_3OH, at the reference state U_{WR} = 2 V, for the sample PdZn/K are represented in Fig. 5. The aim was to find the flow rate required to avoid mass transfer limitation phenomena. The reference (unpromoted) CO_2 reaction rate initially increased with the flow rate, reaching a plateau at 120 ml min^{-1}. The CO_2 conversion decreased in a linear manner upon increasing the flow rate. The methanol selectivity increases at lower CO_2 conversion, this behavior was also found in conventional catalysis [30].

3.3. PdZn/Na electrochemical catalyst

In order to study the catalytic behavior in depth, all samples (PdZn/K, PdZn/Na and PdZn0.13/K) were tested under different reaction conditions and at different potentials (U_{WR}) ranging from +2 V to −2 V. The study of each catalyst separately was necessary due to the differences found in the dynamic response of the reaction rates for each catalyst. It should be noted that for this sample two types of particles are present, namely metallic Pd and PdZn alloy particles, as shown by the results of an XRD analysis. These particles will have a different electrocatalytic behaviors when Na^+ ions migrate to the catalytic film.

The dynamic response of the reaction rates for CO and CH_3OH formation for the catalyst PdZn/Na with a feed composition of 90%

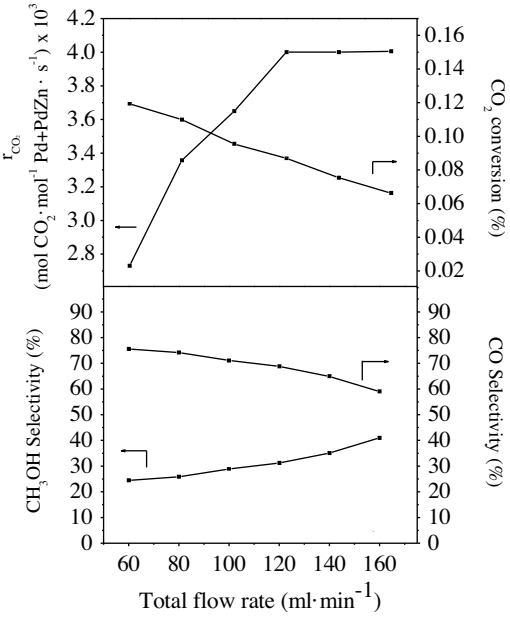

Fig. 5. Effect of the overall gas flow rate on the CO_2 consumption rate, CO_2 conversion and CH_3OH and CO selectivity, under +2 V polarization for the PdZn/K catalyst. Reaction conditions: 10% CO_2 and 90% H_2 at 340 °C.

H_2 and 10% CO_2 at 300 °C is shown in Fig. 6. This sample showed that a low quantity of sodium ions improves the PdZn alloy activity towards methanol (potentials of 0.5 V and −0.5 V) compared to the reference state (2 V). Moreover, it can be seen that the methanol production decreased at lower potentials due to the migration of large amounts of Na^+ onto the catalyst-working electrode, which would weaken the chemical bond between PdZn and Pd and the electron donor adsorbate (H_2) and strengthen the bond with electron acceptors (CO_2). The increase in the binding strength of CO_2 on the PdZn surface would disfavor methanol production because the kinetic is disfavored by lower levels of the adsorbate H_2. At the same time, the increase in the binding strength of CO_2 on the Pd surface would favor the dissociative adsorption of CO_2 through the reverse water gas-shift reaction (Eq. (2)). Therefore electrophilic behavior was obtained for CO because a cathodic (negative) polarization enhanced the carbon monoxide production rate. The highest CO production was obtained at −1 V, where the cathodic peak was found in the cyclic voltammetry study (Fig. 4). From this potential, the CO formation rate showed sharp positive peaks whereas the CH_3OH formation rate showed negative peaks. This behavior is consistent with the results of the cyclic voltammetry analysis. As explained above, the high intensity found in the voltammetry study at −1 V is related to the formation of sodium carbonates and sodium hydrides. These compounds can block the active sites of the catalyst and decrease its activity. The differences found in the values for the formation and decomposition peak areas in the voltammetry study suggest that these species are not totally decomposed after each cycle. This situation is consistent with the catalytic results: the highest CO production rate found at −1 V (where more species are formed) is not obtained at −1.5 V or −2 V due to the blocking effect of the species that are not decomposed. Hence, the trend in the methanol formation rate is opposite to that of the CO formation rate because the kinetic of the latter is favored by the strengthening with the CO_2 (electron acceptor) while the methanol kinetic is disadvantaged. In addition, although CO is formed preferentially, when poisoning in the CO formation rate occurs due to the formation of certain compounds, the blocking produced at the active palladium sites leads to a recovery in the formation rate of methanol because the free H_2 (not used in blocked Pd active sites) migrates to PdZn active sites to produce methanol.

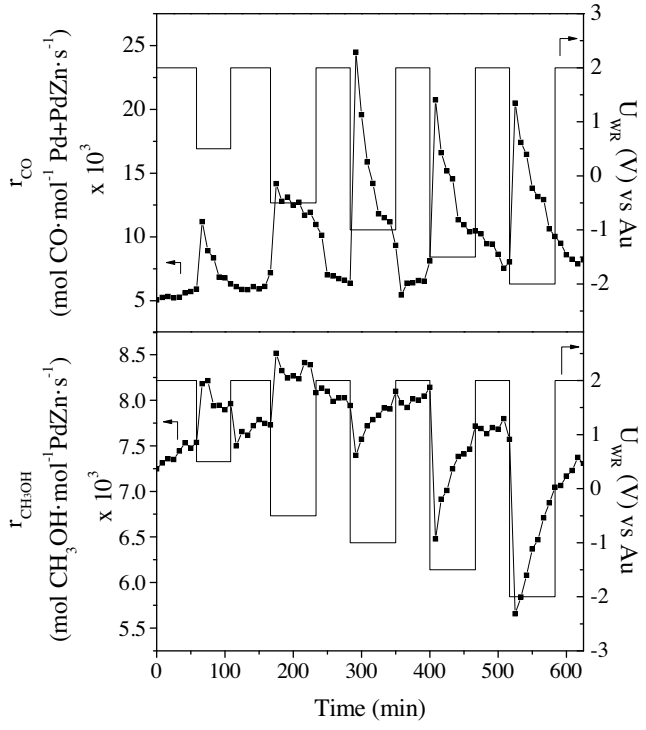

Fig. 6. Influence of the applied potential vs. time on the reaction rate values of CO production and CH_3OH formation for the catalyst PdZn/Na under conditions of 10% CO_2 and 90% H_2 at 300 °C. Total flow rate = 120 ml min^{-1}.

3.4. PdZn/K electrochemical catalyst

The dynamic responses of the reaction rates for CO_2, CO and CH_3OH for the catalyst PdZn/K under all the conditions used in this work are shown in Fig. 7. The reaction rates of CO_2 and CO are fairly similar since the contribution of the CH_3OH formation rate to the total is low. Although methanol is obtained in a lower order of magnitude, the production of this compound is remarkable and this is the first time that a dynamic and stable response has been reported for this product in the hydrogenation of CO_2.

Although the PdZn/Na and PdZn/K samples have similar particle sizes for the Pd and the PdZn alloy, the PdZn/Na sample showed high activity towards methanol and CO. This behavior could be due to the higher amount palladium exposed in the form of PdZn or metallic palladium at the external surface, as shown by EDX analysis in SEM images (Fig. 3). As for the PdZn/Na sample, the methanol formation rate increases at 0.5 V and decreases at lower potentials, whereas electrophilic behavior was found for the carbon monoxide formation rate. When the K^+ ions migrate to the catalytic film, an increase in the CO_2 (electron acceptor) production is observed and, consequently, this change favors CO production and inhibits methanol production. The difference between the promotional effects is that in the case of the PdZn/K sample the effect is stable.

The reaction rates of CO_2 and CO increased with temperature due to the enhancement of the CO reaction (Eq. (2)). When the H_2/CO_2 ratio in the feed atmosphere was decreased, higher reaction rates were obtained for CO and CO_2 but more time was required to return to the value of the unpromoted state (+2 V). In some cases, however, this value was not reached at high temperatures, thus leading to an increase in the global activity of the catalyst. The reaction rate of CH_3OH also increased with temperature at lower H_2/CO_2 ratios (3 and 9), but this was not the case for the 2.5% CO_2/97.5% H_2 mixture. Although the methanol reaction rate increased at +0.5 V, the selectivity towards this compound decreased at this potential (Table 3) due to the increase found for the carbon monoxide reaction rate at +0.5 V. The highest methanol selectivity was found for the highest H_2/CO_2 ratio (39, corresponding to the 2.5% CO_2/97.5% H_2 experiment) at 300 °C and 2 V. The selectivity was around 76% but this decreased to 60% and 41% at the ratios 9 and 3, respectively. Therefore, higher H_2/CO_2 ratios led to higher selectivity towards methanol. In general, the methanol selectivity decreased with the temperature due to the thermodynamical limitations of this reaction and the preferential formation of CO. The optimum of selectivity was found at 300 °C and this is consistent with the equilibrium for methanol production (Eq. (3)), which is favored at lower temperatures.

The variations with applied potential of the CO reaction rate enhancement ratio (ρ_{CO}) and the apparent Faradaic efficiencies for both products, under all the feed compositions and for two temperatures (300 °C and 340 °C), are represented in Fig. 8. The figure also shows the CH_3OH reaction rate enhancement ratio (ρ_{CH3OH}) at the potential +0.5 V, where the ratio is higher than 1. The CO reaction rate enhancement ratio increased at higher H_2/CO_2 ratios, at higher temperature, and at negative potentials, which proves that the latter favors CO_2 adsorption and consequently the kinetic for the production of CO. The highest CH_3OH reaction rate enhancement ratio at 300 °C was found for the conditions 10% CO_2/90% H_2. The efficiency achieved for CO (Λ_{CO} = 3250) is the highest

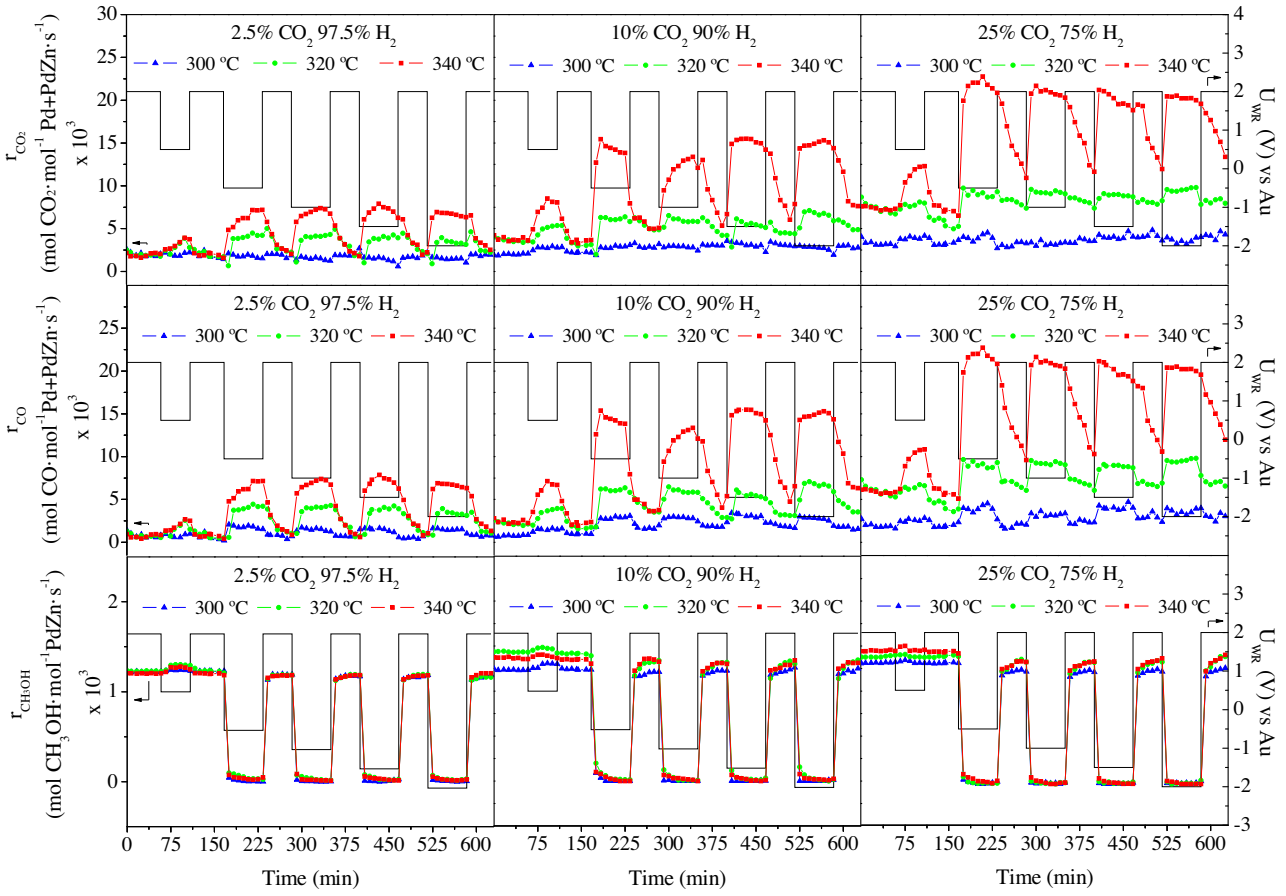

Fig. 7. Influence of the applied potential vs. time on the reaction rate values of CO_2 consumption, CO production and CH_3OH formation for the catalyst PdZn/K under three different feed ratios: 25% CO_2 and 75% H_2, 10% CO_2 and 90% H_2, 2.5% CO_2 and 97.5% H_2 at the temperatures of 300 (blue), 320 (green) and 340 °C (red). Total flow rate = 120 ml min^{-1}. (For interpretation of the references to colour in this figure legend, the reader is referred to the web version of this article.)

value found in the literature for a hydrogenation reaction. For instance, in a recent study [16] Λ values as high as 500 were claimed for the first time but these are significantly lower than the values found in this study. Interestingly, both apparent Faradaic efficiencies exhibit a pronounced maximum with varying anodic potential, as observed in other work [16]. This behavior may be due to the fact that the first migration of potassium ions to the PdZn film is produced easily because it is favored by the concentration gradient of ions. As a consequence, only a very small current is necessary for this process. However, when the potential continues to decrease, the movement of potassium ions becomes more difficult due to the existence of ions on the PdZn film. Thus, higher currents are necessary and this leads to a decrease in the Λ values.

Table 3
Methanol selectivity and CO_2 conversion for the catalyst PdZn/K.

		2.5%CO_2 97.5%H_2		10%CO_2 90%H_2		25%CO_2 75%H_2	
		S_{CH3OH} (%)	X_{CO2} (%)	S_{CH3OH} (%)	X_{CO2} (%)	S_{CH3OH} (%)	X_{CO2} (%)
300 °C	2V	76	0.1	60	<0.1	41	<0.1
	0.5V	54	0.2	45	<0.1	31	<0.1
320 °C	2V	65	0.2	46	<0.1	20	<0.1
	0.5V	33	0.3	25	0.1	17	0.1
340 °C	2V	61	0.2	35	0.1	18	0.1
	0.5V	31	0.3	16	0.2	12	0.1

3.5. PdZn0.13/K electrochemical catalyst

The PdZn0.13/K catalyst was prepared in order to study the influence of the Pd/Zn molar ratio in the catalytic film formed. Two main differences were found during the characterization: (i) a

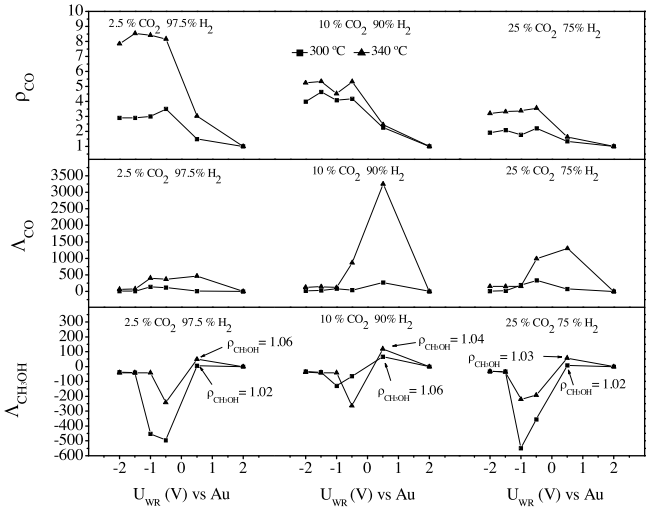

Fig. 8. Effect of the applied potential (UWR) on the rate enhancement ratio (ρi) and on the apparent Faradaic efficiency (Λi) for the catalyst PdZn/K under three different feed ratios: 25% CO_2 and 75% H_2, 10% CO_2 and 90% H_2, 2.5% CO_2 and 97.5% H_2 at the temperatures of 300 and 340 °C. Total flow rate = 120 ml min^{-1}.

different external morphology of the catalyst film (Fig. 3), i.e., less compact, rougher and with small holes and (ii) only PdZn alloy particles were evidenced in the XRD analysis (Fig. 2). The consequence of the first characteristic is that the particles formed were smaller and the dispersion was higher. These differences are essential to understand the catalytic results because, in this case, the electrocatalytic behavior depends only on the PdZn particles and how they act when the migration of K^+ ions is produced.

The dynamic response of the reaction rates for CO and CH_3OH formation for the catalyst PdZn0.13/K with a feed composition of 90% H_2 and 10% CO_2 at 300 °C is shown in Fig. 9. Although this experiment was selected as an example, the experiments carried out under different conditions showed the same trend. This sample shows the same catalytic behavior for both products (CO and CH_3OH). The migration of a small quantity of K^+ ions produced at 0.5 V improves the kinetics of both reactions but at lower potentials (<0.5 V) the migration of K^+ ions to the PdZn film inhibits the global activity of the electrochemical catalyst.

The Pd/Zn molar ratio did not show any influence on methanol production because similar formation rates were obtained for both catalysts (PdZn/K and PdZn0.13/K). The same behavior was also found in other work on conventional catalysts [30], where it was found that a certain number of PdZn alloy particles provide the maximum methanol production regardless of further changes to the Pd/Zn molar ratio. The high CO production rate when compared with the PdZn/K sample occurs because the PdZn particles are smaller and the dispersion is higher, therefore the activity of the catalyst is higher. It was noted that while the methanol reaction rate seems similar in the different cycles (+2 to a negative potential), the carbon monoxide formation rate decreased. Thus, deactivation of the electrochemical catalyst is produced in this process. The authors of this work suggest that the deactivation is produced in PdZn alloy particles. This effect is only evident in CO formation rates because the order of magnitude in which this compound is produced is higher, so the effect of deactivation is

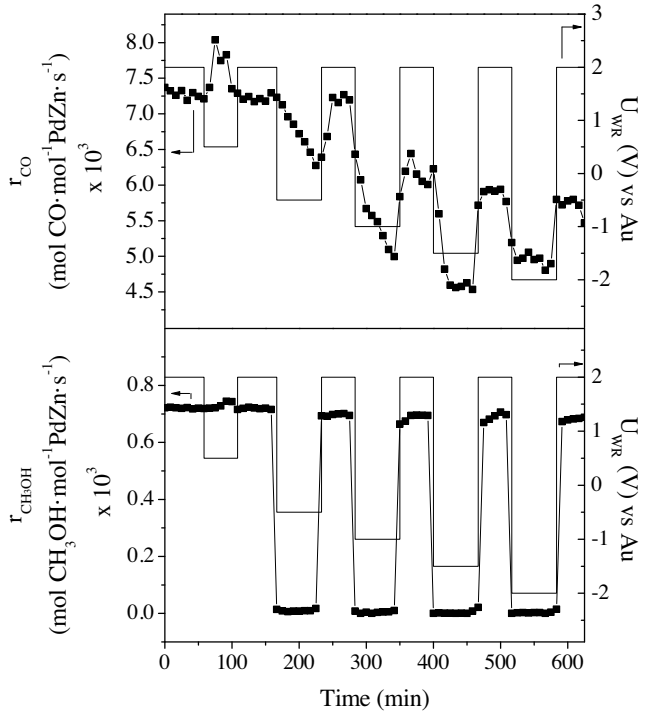

Fig. 9. Influence of the applied potential vs. time on the reaction rate values of CO production and CH_3OH formation for the catalyst PdZn0.13/K under conditions of 10% CO_2 and 90% H_2 at 300 °C. Total flow rate = 120 ml min^{-1}.

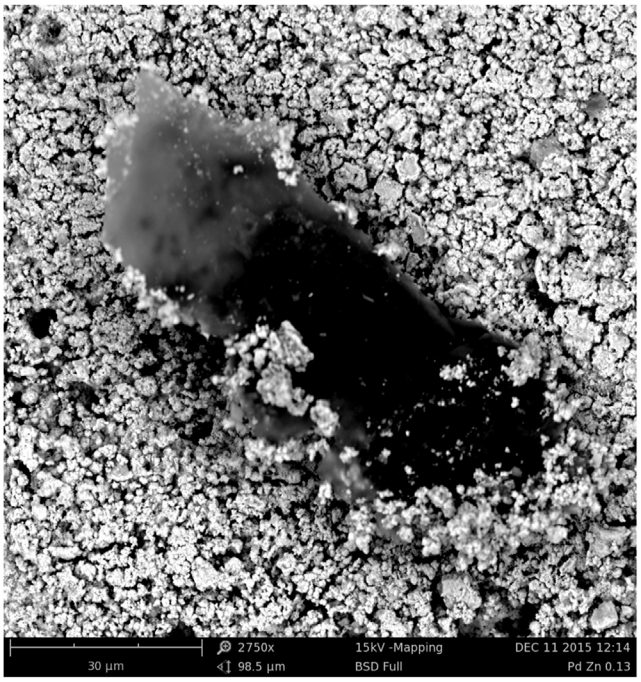

Fig. 10. SEM image of a carbonaceous deposit found on the surface of the PdZn0.13/K sample.

easier to see. Evidence for this phenomenon is provided by the existence of carbonaceous deposits (Fig. 10) on the catalyst surface, with a carbon content greater than 60%. The authors suggest that the deactivation is produced in all of the PdZn alloy particles (also in the hidden particles), but carbonaceous deposits were only found on the surface at the points where the Au wires were connected with the PdZn alloy. This finding is due to the high activity and migration of ions in the vicinity of the connections. The deactivation observed between the first and the last reference state in the CO formation rate is around 25% for all temperatures tested.

4. Conclusions

The following conclusions can be drawn from this study:

- The PdZn alloy can be used as a catalytic film in an electrochemical system. Methanol and carbon monoxide were the two only products obtained.
- The formation of potassium carbonates and potassium hydrides was demonstrated by a cyclic voltammetry study on the sample PdZn0.13/K. The sample PdZn/Na showed high intensities in the cyclic voltammetry study. These values are related to a higher capture of reactants through the formation of sodium compounds.
- PdZn/Na and PdZn/K samples shows how a low quantity of ions increases the formation rate of CH_3OH and a high quantity leads to the poisoning of the PdZn active sites. An electrophilic behavior for the CO formation rate was found. These behaviors are attributed to the coexistence of large particles of metallic palladium and PdZn alloy.
- The PdZn/Na sample showed an unstable promotional effect in the dynamic response. As shown by cyclic voltammetry, sodium carbonates and sodium hydrides are formed and these could block the active sites, thus decreasing the reaction rate.
- The PdZn/K sample showed a stable promotional effect for both products. A complete dynamic study was carried out under different conditions: feed H_2/CO_2 ratios of 3, 9 and 39 and

temperatures of 300, 320 and 340 °C. Apparent Faradaic efficiency values up to 1000 were obtained.

- The PdZn0.13/K sample showed the same catalytic behavior for both products. CO and CH_3OH formation rates increase at +0.5 V compared to the unpromoted state (+2 V) and these decreased at negative potentials. This behavior was attributed to the fact that the EPOC effect in this catalyst is produced in PdZn alloy particles.

Acknowledgements

The authors would like to thank the Ministerio de Economía y Competitividad (project PCIN-2013-183) and the Spanish government (grant FPU13/00727) for their financial support.

References

[1] A.A. Olajire, Valorization of greenhouse carbon dioxide emissions into value-added products by catalytic processes, J. CO_2 Util. 3-4 (2013) 74–92.
[2] K.A. Ali, A.Z. Abdullah, A.R. Mohamed, Recent development in catalytic technologies for methanol synthesis from renewable sources: a critical review, Renew. Sustainable Energy Rev. 44 (2015) 505–518.
[3] S. Saeidi, N.A.S. Amin, M.R. Rahimpour, Hydrogenation of CO_2 to value-added products – A review and potential future developments, J. CO_2 Util. 5 (2014) 66–81.
[4] N. Gutiérrez-Guerra, L. Moreno-López, J.C. Serrano-Ruiz, J.L. Valverde, A. de Lucas-Consuegra, Gas phase electrocatalytic conversion of CO_2 to syn-fuels on Cu based catalysts-electrodes, Appl. Catal. B 188 (2016) 272–282.
[5] K. Sun, Z. Fan, J. Ye, J. Yan, Q. Ge, Y. Li, W. He, W. Yang, C.-j. Liu, Hydrogenation of CO_2 to methanol over In_2O_3 catalyst, J. CO_2 Util. 12 (2015) 1–6.
[6] C. Huang, S. Chen, X. Fei, D. Liu, Y. Zhang, Catalytic hydrogenation of CO_2 to methanol: study of synergistic effect on adsorption properties of CO_2 and H_2 in CuO/ZnO/ZrO_2 system, Catalysts 5 (2015) 1846–1861.
[7] X. Jiang, N. Koizumi, X. Guo, C. Song, Bimetallic Pd-Cu catalysts for selective CO_2 hydrogenation to methanol, Appl. Catal. B 170–171 (2015) 173–185.
[8] M. Saito, R&D activities in Japan on methanol synthesis from CO_2 and H_2, Catal. Surv. Jpn. 2 (1998) 175–184.
[9] S.G. Jadhav, P.D. Vaidya, B.M. Bhanage, J.B. Joshi, Catalytic carbon dioxide hydrogenation to methanol: a review of recent studies, Chem. Eng. Res. Des. 92 (2014) 2557–2567.
[10] A.M. Shulenberger, F.R., Jonsson, O., Ingolfsson, K.C. Tran, Process for producing liquid fuel from carbon dioxide and water, Google Patents, 2012.
[11] A. de Lucas-Consuegra, New trends of alkali promotion in heterogeneous catalysis: electrochemical promotion with alkaline ionic conductors, Catal. Surv. Asia. 19 (2015) 25–37.
[12] M. Stoukides, C.G. Vayenas, The effect of electrochemical oxygen pumping on the rate and selectivity of ethylene oxidation on polycrystalline silver, J. Catal. 70 (1981) 137–146.
[13] C.G. Vayenas, S. Bebelis, S. Ladas, Dependence of catalytic rates on catalyst work function, Nature 343 (1990) 625–627.
[14] C.G. Vayenas, S., Bebelis, C., Pliangos, S., Brosda, D. Tsiplakides, Electrochemical Activation of Catalysis: Promotion, Electrochemical Promotion, and Metal-Support Interactions, Springer US2007.
[15] N. Gutiérrez-Guerra, J. González-Cobos, J.C. Serrano-Ruiz, J.L. Valverde, A. de Lucas-Consuegra, Electrochemical activation of Ni catalysts with potassium ionic conductors for CO_2 hydrogenation, Top. Catal. 58 (2015) 1256–1269.
[16] I. Kalaitzidou, A. Katsaounis, T. Norby, C.G. Vayenas, Electrochemical promotion of the hydrogenation of CO_2 on Ru deposited on a BZY proton conductor, J. Catal. 331 (2015) 98–109.
[17] S. Bebelis, H. Karasali, C.G. Vayenas, Electrochemical promotion of the CO_2 hydrogenation on Pd/YSZ and Pd/β''-Al_2O_3 catalyst-electrodes, Solid State Ionics 179 (2008) 1391–1395.
[18] E. Ruiz, D. Cillero, P.J. Martínez, Á. Morales, G.S. Vicente, G. de Diego, J.M. Sánchez, Bench scale study of electrochemically promoted catalytic CO_2 hydrogenation to renewable fuels, Catal. Today 210 (2013) 55–66.
[19] E. Ruiz, D. Cillero, P.J. Martínez, Á. Morales, G.S. Vicente, G. de Diego, J.M. Sánchez, Electrochemical synthesis of fuels by CO_2 hydrogenation on Cu in a potassium ion conducting membrane reactor at bench scale, Catal. Today 236 (Part A) (2014) 108–120.
[20] D. Theleritis, M. Makri, S. Souentie, A. Caravaca, A. Katsaounis, C.G. Vayenas, Comparative study of the electrochemical promotion of CO_2 hydrogenation over Ru-Supported catalysts using electronegative and electropositive promoters, ChemElectroChem 1 (2014) 254–262.
[21] M. Makri, A. Katsaounis, C.G. Vayenas, Electrochemical promotion of CO_2 hydrogenation on Ru catalyst-electrodes supported on a K-β''-Al_2O_3 solid electrolyte, Electrochim. Acta 179 (2015) 556–564.
[22] E.I. Papaioannou, S. Souentie, A. Hammad, C.G. Vayenas, Electrochemical promotion of the CO_2 hydrogenation reaction using thin Rh, Pt and Cu films in a monolithic reactor at atmospheric pressure, Catal. Today 146 (2009) 336–344.
[23] S. Bebelis, H. Karasali, C.G. Vayenas, Electrochemical promotion of CO_2 hydrogenation on Rh/YSZ electrodes, J. Appl. Electrochem. 38 (2008) 1127–1133.
[24] V. Jiménez, C. Jiménez-Borja, P. Sánchez, A. Romero, E.I. Papaioannou, D. Theleritis, S. Souentie, S. Brosda, J.L. Valverde, Electrochemical promotion of the CO_2 hydrogenation reaction on composite Ni or Ru impregnated carbon nanofiber catalyst-electrodes deposited on YSZ, Appl. Catal. B 107 (2011) 210–220.
[25] E. Ruiz, D. Cillero, P.J. Martínez, Á. Morales, G.S. Vicente, G. de Diego, J.M. Sánchez, Bench-scale study of electrochemically assisted catalytic CO_2 hydrogenation to hydrocarbon fuels on Pt, Ni and Pd films deposited on YSZ, J. CO_2 Util. 8 (2014) 1–20.
[26] D. Theleritis, S. Souentie, A. Siokou, A. Katsaounis, C.G. Vayenas, Hydrogenation of CO_2 over Ru/YSZ electropromoted catalysts, ACS Catal. 2 (2012) 770–780.
[27] G. Pekridis, K. Kalimeri, N. Kaklidis, E. Vakouftsi, E.F. Iliopoulou, C. Athanasiou, G.E. Marnellos, Study of the reverse water gas shift (RWGS) reaction over Pt in a solid oxide fuel cell (SOFC) operating under open and closed-circuit conditions, Catal. Today 127 (2007) 337–346.
[28] G. Karagiannakis, S. Zisekas, M. Stoukides, Hydrogenation of carbon dioxide on copper in a H^+ conducting membrane-reactor, Solid State Ionics 162–163 (2003) 313–318.
[29] J. Díez-Ramírez, J.L. Valverde, P. Sánchez, F. Dorado, CO_2 Hydrogenation to Methanol at atmospheric pressure: influence of the preparation method of Pd/ZnO catalysts, Catal. Lett. 146 (2016) 373–382.
[30] J. Díez-Ramírez, P. Sanchez, A. Rodríguez-Gomez, J.L. Valverde, F. Dorado, Carbon nanofiber-based palladium/zinc catalysts for the hydrogenation of carbon dioxide to methanol at atmospheric pressure, Ind. Eng. Chem. Res. 55 (2016) 3556–3567.
[31] Y.H. Chin, Y. Wang, R.A. Dagle, X.S. Li, Methanol steam reforming over Pd/ZnO: Catalyst preparation and pretreatment studies, Fuel. Process. Technol. 83 (2003) 193–201.
[32] Y.H. Chin, R. Dagle, J. Hu, A.C. Dohnalkova, Y. Wang, Steam reforming of methanol over highly active Pd/ZnO catalyst, Catal. Today 77 (2002) 79–88.
[33] Y. Wang, J. Zhang, H. Xu, Interaction between pd and ZnO during reduction of Pd/ZnO catalyst for steam reforming of methanol to hydrogen, Chin. J. Catal. 27 (2006) 217–222.
[34] N. Iwasa, T. Mayanagi, N. Ogawa, K. Sakata, N. Takezawa, New catalytic functions of Pd-Zn, Pd-Ga Pd-In, Pt-Zn, Pt-Ga and Pt-In alloys in the conversions of methanol, Catal. Lett. 54 (1998) 119–123.
[35] H. Zhang, J. Sun, V.L. Dagle, B. Halevi, A.K. Datye, Y. Wang, Influence of ZnO facets on Pd/ZnO catalysts for methanol steam reforming, ACS Catal. 4 (2014) 2379–2386.
[36] N. Iwasa, S. Masuda, N. Ogawa, N. Takezawa, Steam reforming of methanol over Pd/ZnO: effect of the formation of PdZn alloys upon the reaction, Appl. Catal. A 125 (1995) 145–157.
[37] A. de Lucas-Consuegra, N. Gutiérrez-Guerra, A. Caravaca, J.C. Serrano-Ruiz, J.L. Valverde, Coupling catalysis and electrocatalysis for hydrogen production in a solid electrolyte membrane reactor, Appl. Catal. A 483 (2014) 25–30.
[38] N.H. Iwasa Suzuki, M. Terashita, N. Arai, Methanol synthesis from CO_2 under atmospheric pressure over supported Pd catalysts, Catal. Lett. 96 (2004) 75–78.
[39] N.C. Filkin, M.S. Tikhov, A. Palermo, R.M. Lambert, A kinetic and spectroscopic study of the in situ electrochemical promotion by sodium of the platinum-catalyzed combustion of propene, J. Phys. Chem. A 103 (1999) 2680–2687.
[40] P. Vernoux, F. Gaillard, C. Lopez, E. Siebert, In-situ electrochemical control of the catalytic activity of platinum for the propene oxidation, Solid State Ionics 175 (2004) 609–613.
[41] E. Ruiz, D. Cillero, Á. Morales, G.S. Vicente, G. de Diego, P.J. Martínez, J.M. Sánchez, Bench-scale study of electrochemically promoted CO_2 capture on Pt/K-βAl_2O_3, Electrochim. Acta 112 (2013) 967–975.
[42] A.J. Urquhart, J.M. Keel, F.J. Williams, R.M. Lambert, Electrochemical promotion by potassium of rhodium-catalyzed Fischer-Tropsch synthesis: XP spectroscopy and reaction studies, J. Phys. Chem. B 107 (2003) 10591.
[43] P. Vernoux, F. Gaillard, C. Lopez, E. Siebert, In-situ electrochemical control of the catalytic activity of platinum for the propene oxidation, Solid State Ionics 175 (2004).
[44] A. de Lucas-Consuegra, F. Dorado, J.L. Valverde, R. Karoum, P. Vernoux, Low-temperature propene combustion over Pt/K-βAl2O3 electrochemical catalyst: characterization, catalytic activity measurements, and investigation of the NEMCA effect, J. Catal. 251 (2007) 474–484.